0 0 0 0 4 9 0 2 4 3 1

UC-32
UC-38

Submitted to Tectonophysics

LBL-6912
Preprint

FLUID DYNAMICS MODEL FOR SALT-DOME EVOLUTION

N. E. Nasir and O. B. Dabbousi

RECEIVED
LAWRENCE
BERKELEY LABORATORY

NOV 8 1977

LIBRARY AND
DOCUMENTS SECTION

August 1977

Prepared for the U. S. Energy Research and
Development Administration under Contract W-7405-ENG-48

For Reference

Not to be taken from this room

LBL-6912 c.1

LEGAL NOTICE

This report was prepared as an account of work sponsored by the United States Government. Neither the United States nor the Department of Energy, nor any of their employees, nor any of their contractors, subcontractors, or their employees, makes any warranty, express or implied, or assumes any legal liability or responsibility for the accuracy, completeness or usefulness of any information, apparatus, product or process disclosed, or represents that its use would not infringe privately owned rights.

0 0 0 0 4 9 0 2 4 3 2

LBL-6912

FLUID DYNAMICS MODEL FOR SALT-DOME EVOLUTION

N. E. Nasir

Department of Mathematics
University of Petroleum and Minerals
Dhahran, Saudi Arabia

and

O. B. Dabbousi

Materials and Molecular Research Division
Lawrence Berkeley Laboratory
University of California
Berkeley, California 94720

and

Department of Physics
University of Petroleum and Minerals
Dhahran, Saudi Arabia*

ABSTRACT

A fluid dynamics model for the evolution of salt domes and ridges is presented. The model assumes a rigid substrate, finite thickness of both strata with no slip and a rigid or free surface of overburden. Inertial terms in the Navier-Stokes equations are neglected due to the large viscosities considered and the initial perturbation is taken to be sinusoidal. Finite sine and cosine transforms are used to solve the flow equations and the resulting systems of equations reproduces the velocity field equation of Ramberg's model. Assuming an initial interface, the infinite series solution is truncated to obtain the constants of the integration from the boundary conditions. The interface is then moved to a new position. Thus, the new shape for the interface can be traced for any time.

For small perturbations, we obtain results that are approximately those obtained by the linear theory. Results of the numerical solution of the model for both large and small perturbations are presented.

---

* Permanent address.

1. INTRODUCTION

The relative high mobility of saline rock, particularly the evolution of salt-domes and ridges, renders salt-dome tectonics as an example for the tectonic evolution of many geological and geophysical phenomena. In most of these phenomena, a gravitational instability is the underlying cause. A gravitational instability will result whenever a lower density material is overlain with a higher density material. This observation was demonstrated experimentally by Parker and McDonnell, 1955, who also found that this process is independent of the value of the viscosities of the materials. Many theoretical treatments for the gravitational instabilities of layered systems, as well as experimental results, have also been reported in the literature for a long time, e.g., Rayleigh, 1883; Chandrasekhar, 1955; Biot, 1961; Daneš, 1964; Biot and Odé, 1965; Ramberg, 1967, 1968a, 1968b, 1972a, 1972b; and Berner et al, 1972).

Lord Rayleigh, in 1883, considered a periodic disturbance in an incompressible heavy fluid of variable density horizontally stratified. He found that for the case of two uniform fluids of densities ρ_1 and ρ_2 (the subscripts 1 and 2 refer to the upper and lower fluids respectively) separated by a common boundary, the amplitude of the disturbance grows proportional to $e^{\alpha t}$, where

$$\alpha^2 = gk \frac{(\rho_1 - \rho_2)}{(\rho_1 + \rho_2)} , \tag{1.1}$$

k denotes the wave number of the disturbance considered, and g is the acceleration of gravity. Thus, if $\rho_1 > \rho_2$ [in Eq. (1.1)], α^2 is positive and the magnitude of the disturbance grows unbounded with the smallest λ growing the fastest. Hence, the system would be physically unstable.

However, if $\rho_2 > \rho_1$ the α is imaginary and the solution is periodic (Allred and Blount, 1954).

The above simple results were for perfect fluids with neglect of the viscosities, surface tension, and quadratic terms in the velocities. Pennington and Bellman, 1952, and Birkhoff and Ingraham, 1952, discussed these effects on Taylor instabilities (Taylor, 1950) and showed that surface tension does affect the nature of the instability. In essence, the surface tension puts a limit on the wave number and slows the instability. However, it is unlikely that surface tension plays a significant role in any of the physical systems which are of interest geologically and for which we shall seek a solution; hence, surface tension effect will be neglected.

To discuss the effects of viscosity on the motion of the interface in a multilayered system we start with the general fluid flow equation and consider a simple configuration which consists of two horizontal layers of homogeneous materials of density ρ_1 and ρ_2 and viscosity η_1 and η_2, resting on a rigid base. The interference between the two layers normal to the direction of the gravitational force is subjected to a perturbation of given period and small amplitude (Fig. 1).

If the densities are constant, then the equation of continuity for either fluid becomes

$$\nabla \cdot (\vec{u}_i) = 0 , \qquad i = 1 \text{ or } 2 , \tag{1.2}$$

and the equations of motion become the Navier-Stokes equation (Landau and Lifshitz, 1959; and Berker, 1963)

$$\frac{d\vec{u}_i}{dt} - \gamma\nabla^2(\vec{u}_i) = F - \frac{1}{\rho_1}\nabla P_i . \tag{1.3}$$

In two dimensions these equations reduce to

$$\left.\begin{aligned} \rho_i \frac{du_i}{dt} - \eta_i \nabla^2 u_i &= -\frac{\partial P_i}{\partial x} \\ \rho_i \frac{dv_i}{dt} - \eta_i \nabla^2 v_i &= -\rho_i g - \frac{\partial P_i}{\partial y} \\ \frac{\partial u_i}{\partial x} + \frac{\partial v_i}{\partial y} &= 0 \end{aligned}\right\} \quad i = 1 \text{ or } 2 , \tag{1.4}$$

where u and v are the x and y components of the particle velocity, respectively, and P is the internal pressure.

The set of equations (1.4) is nonlinear due to the convective terms that appear in the total time derivatives du/dt and dv/dt. A solution subject to the simplest boundary conditions is very difficult to find. If, however, we neglect all these nonlinearities, then u and v will satisfy the biharmonic equation and will possess well known solutions:

$$\left.\begin{aligned} \nabla^2 \left(\eta_i \nabla^2 - \rho_i \frac{\partial}{\partial t}\right)(u_i, v_i) &= 0 \\ \text{and} \qquad \frac{\partial u_i}{\partial x} + \frac{\partial v_i}{\partial y} &= 0 \end{aligned}\right\} \quad i = 1 \text{ or } 2 . \tag{1.5}$$

One can further show that P will satisfy Laplace's equation with

$$\nabla^2 P = 0 \tag{1.6}$$

Other nonlinearities appear in the boundary conditions at the interface. In many previous works on the motion of the interface, this boundary condition has been linearized (Harrison, 1908; Lamb, 1945; Chandrasekhar, 1955; Biot, 1961; Odé, 1966).

To examine this linearization, we let a perturbation $y = y_1(x,t)$ be given, then

$$\frac{dy}{dt} = u\frac{\partial y_1}{\partial x} + \frac{\partial y_1}{\partial t} \quad ;$$

therefore,

$$\frac{\partial y_1}{\partial t} = v - u\frac{\partial y_1}{\partial x} \quad . \tag{1.7}$$

If $\partial y_1/\partial x$ (the slope of the interface) is small, it is sufficient to write

$$\frac{\partial y_1}{\partial t} = v \quad , \tag{1.8}$$

which means that the new velocity is evaluated at the old interface, and the perturbation must be small.

In the present work, we study the motion of the interface while including the slope of the interface in the boundary condition (see Appendix A).

2. BOUNDARY CONDITIONS

Because of the periodicity of the initial perturbation we confine the study of the development of the interface to a single half wave, that is, part ABCDEF in Fig. 1. In this region we assume that the Navier-Stokes equations hold and that the boundary conditions are as follows:

1) On the vertical sides AFE and BCD, $u_i = 0$, and $\partial v_i/\partial x = 0$. This choice of condition is compatible with the periodicity of the perturbation.

2) On the bottom ED, $u_2 = v_2 = 0$. Particles next to a rigid surface usually adhere to it and do not move.

3) On the top AB, one of two conditions may be used:

   a) A rigid top in which case $u_1 = v_1 = 0$.

   b) A free surface where the tangential viscous drag and the normal viscous force are zero.

$$\sigma_{xy} = \eta_1 \left(\frac{\partial v_1}{\partial x} + \frac{\partial u_1}{\partial y} \right) = 0 \qquad \text{at } y = 0$$

$$\sigma_{yy} = 2\eta_1 \frac{\partial v_1}{\partial y} - P_1 = 0 \qquad \text{at } y = 0$$

For simplicity we choose part a) of condition 3); though neither case presents any mathematical complications.

4) At the interface, continuity of viscous forces and particle velocities is required (no slip), i.e.,

$$u_1 = u_2$$

$$v_1 = v_2$$

and

$$(P_2 - P_1) \sin 2\beta = \eta_1 \left(\frac{\partial v_1}{\partial x} + \frac{\partial u_1}{\partial y} \right) - \eta_2 \left(\frac{\partial v_1}{\partial x} + \frac{\partial u_1}{\partial y} \right)$$

$$(P_2 - P_1) \cos 2\beta = -2\eta_1 \frac{\partial v_1}{\partial y} + 2\eta_2 \frac{\partial v_2}{\partial y}$$

where $\beta = \beta(x)$ is the angle the tangent to the interface makes with horizontal. (See Appendix A for the derivation of the fourth boundary condition.)

3. MATHEMATICAL PROCEDURES

The total derivatives du_1/dt and dv_1/dt in Eqs. (1.4) contain convective terms which are the products of velocities and velocity gradients as well as inertial terms. For the physical system under consideration these products are extremely small and therefore negligible. An example of this comes from the calculation of the motion of the interface between two high-viscosity fluids. The velocities we shall neglect were found by Odé, 1966, to be of the order of 1 millimeter/100 years. Thus, it is reasonable to neglect inertial terms relative to viscous forces, and the equations describing the system become

$$\left.\begin{aligned} \eta_i \nabla^2 u_i &= \frac{\partial P_i}{\partial x} \\ \eta_i \nabla^2 v_i &= \rho_i g + \frac{\partial P_i}{\partial y} \\ \frac{\partial u_i}{\partial x} + \frac{\partial v_i}{\partial y} &= 0 \end{aligned}\right\} \quad i = 1 \text{ or } 2 \tag{3.1}$$

The boundary conditions for this system are those given above and may be inferred from Fig. 2.

Now, since $u_i = 0$, and $\partial v_i/\partial x = 0$ on the boundary of a finite region, we may apply the finite sine transform on u_i, and the finite cosine transform on v_i (Erdélyi, 1954). In the following we take $\overline{P}_i = \rho_i g y + p_i$ and $k_n = \pi n/a$, $n = 1,2,3,\ldots$. Therefore, we define

$$u_{is} = \int_0^a u_i \sin k_n x dx \tag{3.2}$$

and

$$v_{ic} = \int_0^a v_i \cos k_n x \, dx \tag{3.3}$$

and

$$P_{ic} = \int_0^a \overline{P}_i \cos k_n x \, dx \quad . \tag{3.4}$$

Next we multiply the u_i equation by $\sin k_n x$, the v_i equation by $\cos k_n x$, and integrate over the interval [0,a]; thus, we have

$$\int_0^a \frac{\partial^2 u_i}{\partial y^2} \sin k_n x \, dx + \int_0^a \frac{\partial^2 u_i}{\partial x^2} \sin k_n x \, dx = \frac{1}{\eta_i} \int_0^a \frac{\partial \overline{P}_i}{\partial x} \sin k_n x \, dx \; . \tag{3.5}$$

Integrating the second integral by parts twice, and using the fact that $u_i = 0$ at $x = 0$ and $x = a$, we obtain

$$\int_0^a \frac{\partial^2 u_i}{\partial x^2} \sin k_n x \, dx = -k_n^2 \int_0^a u_i \sin k_n x \, dx = -k_n^2 u_{is} \; . \tag{3.6}$$

Integrating the right-hand side of Eq. (3.5), we have

$$\frac{1}{\eta_i} \int_0^a \frac{\partial P_i}{\partial x} \sin k_n x \, dx = -\frac{k_n}{\eta_i} \int_0^a P_i \cos k_n x \, dx = -\frac{k_n}{\eta_i} P_{ic} \; . \tag{3.7}$$

Finally, Eq. (3.5) transformed becomes

$$\frac{d^2 u_{is}}{dy^2} - k_n^2 u_{is} = -\frac{k_n}{\eta_i} P_{ic} \; . \tag{3.8}$$

Similarly, the v_i equation and the continuity equation transformed become

$$\frac{d^2 v_{ic}}{dy^2} - k_n^2 v_{ic} = \frac{1}{\eta_i} \frac{dP_{ic}}{dy} \tag{3.9}$$

and

$$\frac{dv_{ic}}{dy} + ku_{is} = 0 \quad . \tag{3.10}$$

Eliminating P_{ic} and u_{is} from Eqs. (3.8), (3.9), and (3.10), we obtain

$$\left(\frac{d^2}{dy^2} - k_n^2\right)^2 v_{ic} = 0 \quad . \tag{3.11}$$

The general solution of Eq. (3.11) is

$$v_{ic}(y,n) = (A_i + B_i k_n y)e^{k_n y} + (C_i + D_i k_n y)e^{-k_n y} \quad , \tag{3.12}$$

where A_i, B_i, C_i, and D_i are constants of integration.

Differentiating Eq. (3.12) with respect to y and substituting the result in Eq. (3.10) we obtain a solution for u_{is},

$$u_{is}(y,n) = (C_i - D_i + D_i k_n y)e^{-k_n y} - (A_i + B_i + B_i k_n y)e^{k_n y} \quad . \tag{3.13}$$

Employing Eqs. (3.13) and (3.8) we obtain a solution for P_{ic},

$$P_{ic}(y,n) = 2\eta_i (B_i k_n e^{k_n y} + D_i k_n e^{-k_n y}) \quad . \tag{3.14}$$

In order to obtain the solutions v_i, u_i, and $\overline{P}_i$ from the solution of the transforms v_{ic}, u_{is}, and P_{ic}, we use the inversion formulae, bearing in mind that v_{ic} and P_{ic} are cosine transforms and that the zeroth term must be treated separately; thus

$$v_i = \frac{1}{a} v_{ic}(y,0) + \frac{2}{a} \sum_{n=1}^{\infty} v_{ic}(y,n) \cos k_n x \quad , \tag{3.15}$$

$$u_i = \frac{2}{a}\sum_{n=1}^{\infty} u_{is}(y,n) \sin k_n x \quad , \tag{3.16}$$

and

$$\overline{P}_i = \frac{1}{a} P_{ic}(y,0) + \frac{2}{a}\sum_{n=1}^{\infty} P_{ic}(y,n) \cos k_n x \quad . \tag{3.17}$$

To evaluate $v_{ic}(y,0)$ we employ the equation of continuity as well as the boundary condition on v_i, for instance,

$$\frac{\partial v_i}{\partial y} = \frac{1}{a}\frac{dv_{ic}(y,0)}{dy} + \frac{2}{a}\sum_{n=1}^{\infty}\frac{dv_{ic}(y,n)}{dy}\cos k_n x \quad ,$$

$$\frac{\partial u_i}{\partial x} = \frac{2}{a}\sum_{n=1}^{\infty} k_n u_{is}(y,n) \cos k_n x \quad .$$

By adding the last two equations, we obtain

$$\frac{\partial v_i}{\partial y} + \frac{\partial u_i}{\partial x} = \frac{1}{a}\frac{dv_{ic}(y,0)}{dy} + \frac{3}{a}\sum_{n=1}^{\infty}\left[\frac{dv_{ic}(y,n)}{dy} + k_n u_{is}\right]\cos k_n x \ . \tag{3.18}$$

The left-hand side of Eq. (3.18) is the continuity equation and it is equal to zero. The bracketed quantity on the right-hand side is, by Eq. (3.10) equal to zero. Therefore,

$$\frac{1}{a}\frac{dv_{ic}(y,0)}{dy} = 0$$

or

$$v_{ic}(y,0) = K_i \quad , \qquad i = 1 \text{ or } 2 \quad \text{and} \quad K = \text{a constant} \ .$$

To evaluate the constants K_i, we must consider the two regions. At the bottom where $y = -h$, the boundary condition is $v_2 = 0$; the transform of

$v_2(-h,x) = 0$, gives $v_{2c}(-h,n) = 0$ for any n; hence,

$$v_{2c}(y,0) = K_2 = 0 \quad . \tag{3.19}$$

In the upper region there are two cases corresponding to the third boundary condition. Case (a), where $v_1(0,x) = 0$, gives by the same argument as above

$$v_{1c}(y,0) = K_1 = 0 \quad . \tag{3.20}$$

In case (b), where the derivative $\partial v_1/\partial y$ is given, $v_{1c}(y,0)$ is still a constant K_1, but not necessarily zero. As pointed out in Section 1, we choose the free surface to be rigid, i.e., $v_1(0,x) = 0$.

To evaluate $P_{ic}(y,0)$ we employ the original differential equation in v_i; this gives

$$\frac{2}{a}\sum_{n=1}\left[\frac{d^2 v_{ic}}{dy^2} - k_n v_{ic} - \frac{1}{\eta_i}\frac{dP_{ic}}{dy}\right]\cos k_n x = \frac{1}{a\eta_i}\frac{dP_{ic}(y,0)}{dy} \quad .$$

The bracketed quantity, in view of Eq. (3.9), is equal to zero; therefore

$$P_{ic}(y,0) = H_i \quad , \qquad i = 1 \text{ or } 2 \text{ and } H \text{ is a constant} \quad .$$

To evaluate the constants H_i, both regions must again be considered. The boundary condition at the top gives $\overline{P}_1(0,x) = 0$; hence,

$$P_{1c}(y,0) = H_1 = 0 \tag{3.21}$$

At the bottom there are no <u>a priori</u> boundary conditions on $\overline{P}$; however, it is logical to assume that in the absence of any perturbation and viscosity the pressure at the bottom should reduce to the hydrostatic head. Therefore,

$$P_2 + \rho_2 gy = P_{2c}(y,0) = H_2 \quad ,$$

Since $P_2(-h,x)$ must be the hydrostatic head, then

$$\rho_2 gh_2 + \rho_2 gh_2 - \rho_2 gh = H_2 \quad ,$$

where h_1 and h_2 are the thicknesses of the two layers, respectively, and $h = h_1 + h_2$; therefore,

$$H_2 = (\rho_1 - \rho_2)gh_1 \tag{3.22}$$

Using Eqs. (3.19) through (3.22) in Eqs. (3.15), (3.16), and (3.17), and rewriting the solutions in their domain of applicability, we obtain

$$v_1 = \frac{2}{a}\sum_{n=1}^{\infty} \cos k_n x \left\{ (A_{1n} + B_{1n}k_n y)e^{k_n y} + (C_{1n} + D_{1n}k_n y)e^{-k_n y} \right\} , \tag{3.23}$$

$$u_1 = \frac{2}{a}\sum_{n=1}^{\infty} \sin k_n x \left\{ (C_{1n} - D_{1n} + D_{1n}k_n y)e^{-k_n y} - (A_{1n} + B_{1n} + B_{1n}k_n y)e^{k_n y} \right\}, \tag{3.24}$$

$$P_1 = \frac{4\eta_1}{a}\sum_{n=1}^{\infty} \cos k_n x \left\{ B_{1n}k_n e^{k_n y} + D_{1n}k_n e^{-k_n y} \right\} - \rho_1 gy \quad , \tag{3.25}$$

$$v_2 = \frac{2}{a}\sum_{n=1}^{\infty} \cos k_n x \left\{ (A_{2n} + B_{2n}k_n y)e^{k_n y} + (C_{2n} + D_{2n}k_n y)e^{-k_n y} \right\}, \tag{3.26}$$

$$u_2 = \frac{2}{a}\sum_{n=1}^{\infty} \sin k_n x \left\{ (C_{2n} - D_{2n} + D_{2n}k_n y)e^{-k_n y} - (A_{2n} + B_{2n} + B_{2n}k_n y)e^{k_n y} \right\} , \tag{3.27}$$

$$P_2 = \frac{4\eta_2}{a}\sum_{n=1}^{\infty}\cos k_n x \left\{ B_{2n}k_n e^{k_n y} + D_{2n}k_n e^{-k_n y} \right\} - \rho_2 gy + (\rho_1 - \rho_2)gh_1 \ . \tag{3.28}$$

The above equations for u_i and v_i have the same form as those derived in the Ramberg theory (Ramberg, 1968a; Berner, 1972) using stream function for incompressible viscous fluid. However, in the Ramberg theory only the dominant mode is retained.

Next we use boundary conditions to find relations between the constants of integration. At the top, $y = 0$ and $u_1 = v_1 = 0$; hence, for any n

$$u_1 = 0 \quad \text{gives} \quad C_{1n} - D_{1n} - A_{1n} + B_{1n} = 0$$

and

$$v_1 = 0 \quad \text{gives} \quad A_{1n} + C_{1n} = 0 \ ;$$

therefore,

$$\left.\begin{aligned} A_{1n} &= -C_{1n} \\ B_{1n} &= 2C_{1n} - D_{1n} \end{aligned}\right\} \tag{3.29}$$

In the lower medium at $y = -h$, $u_2 = v_2 = 0$; hence, for any n

$$u_2 = 0 \quad \text{gives} \quad (C_{2n} - D_{2n} - D_{2n}k_n h)e^{k_n h} - (A_{2n} + B_{2n} - B_{2n}k_n h)e^{-k_n h} = 0$$

and

$$v_2 = 0 \quad \text{gives} \quad (C_{2n} - D_{2n}k_n h)e^{k_n h} + (A_{2n} - B_{2n}k_n h)e^{-k_n h} = 0 \ ;$$

therefore,

$$\left.\begin{aligned} A_{2n} &= (2C_{2n}kh - C_{2n} - 2D_{2n}k^2h^2)e^{2k_n h} \ , \\ B_{2n} &= (2C_{2n} - D_{2n} - 2D_{2n}k_n h)e^{2k_n h} \ . \end{aligned}\right\} \tag{3.30}$$

The relations contained in Eqs. (3.29) and (3.30) reduce the eight sets of unknowns appearing in Eqs. (3.23) through (3.28) to four sets, and upon substitution we have,

$$v_1 = \frac{2}{a}\sum_{n=1}^{\infty} \cos k_n x \left\{ C_{1n}(2k_n y e^{k_n y} - 2 \sinh k_n y) - D_{1n} 2k_n y \sinh k_n y \right\}, \tag{3.31}$$

$$u_1 = \frac{2}{a}\sum_{n=1}^{\infty} \sin k_n x \left\{ C_{1n}(-2k_n y e^{k_n y} - 2 \sinh k_n y) + D_{1n}(2 \sinh k_n y + 2k_n y \cosh k_n y) \right\}, \tag{3.32}$$

$$P_1 = \frac{4\eta_1}{a}\sum_{n=1}^{\infty} \cos k_n x \left\{ C_{1n} 2k_n e^{k_n y} - D_{1n} 2k_n \sinh k_n y \right\} - \rho_1 g y \quad , \tag{3.33}$$

$$v_2 = \frac{2}{a}\sum_{n=1}^{\infty} \cos k_2 x \left\{ C_{2n}\, e^{k_n h}\left[2k_n(h+y)e^{k_n(h+y)} - 2 \sinh k_n(h+y)\right] - D_{2n} e^{k_n h}\left[2k_n^2 h(h+y)e^{k_n(h+y)} + 2k_n y \sinh k_n(h+y)\right] \right\} \tag{3.34}$$

$$u_2 = \frac{2}{a}\sum_{n=1}^{\infty} \sin k_n x \left\{ C_{2n} e^{k_n y}\left[-2 \sinh k_n(h+y) - 2k_n(h+y)e^{k_n(h+y)}\right] + D_{2n} e^{k_n h}\left[2k_n y \cosh k_n(h+y) + 2 \sinh k_n(h+y) + 2k_n h\left(k_n(h+y) + 1\right) e^{k_n(h+y)}\right] \right\} \tag{3.35}$$

$$P_2 = \frac{4\eta_2}{a}\sum_{n=1}^{\infty} \cos k_n x \left\{ C_{2n} e^{k_n h}\, 2k_n e^{k_n(h+y)} - D_{2n} e^{k_n h}\left[2k_n \sinh k_n(h+y) + 2k_n^2 h\, e^{k_n(h+y)}\right] \right\} - \rho_2 g y + (\rho_1 - \rho_2) g h_1 \tag{3.36}$$

The above equations satisfy the set of differential equations (3.1) and the boundary conditions 1), 2), and 3); however, since they contain four sets of an infinite number of unknowns, the boundary condition at the interface will furnish four independent relations between these sets of unknowns.

Let us reexamine the boundary condition at the interface. The kinematic condition valid for a moving interface, $F(x,y,t) = 0$, is that the velocity of a particle in the interface must be tangential to the interface; or, equivalently, that the normal component of the fluid velocity is equal to the normal velocity of the surface itself; otherwise, we should have finite flow of fluid across it. This condition is expressed by $dF/dt = 0$, while these conditions are still valid. In addition, we assume a no-slip condition at the interface to insure continuity of velocities and stresses; therefore, at $y = y_1$, where y_1 is the ordinate of the interface,

$$\left.\begin{aligned} u_1 &= u_2 \\ v_1 &= v_2 \end{aligned}\right\} \tag{3.37}$$

and

$$\left.\begin{aligned} (P_2 - P_1)\sin 2\beta &= \eta_1\left(\frac{\partial u_1}{\partial y} + \frac{\partial v_1}{\partial x}\right) - \eta_2\left(\frac{\partial u_2}{\partial y} + \frac{\partial v_2}{\partial x}\right) \\ (P_2 - P_1)\cos 2\beta &= 2\eta_2\frac{\partial v_2}{\partial y} - 2\eta_1\frac{\partial v_1}{\partial y} \quad , \end{aligned}\right\} \tag{3.38}$$

where $\beta = \beta(x)$ is the angle between the tangent to the interface and the horizontal.

Equations (3.37) and (3.38) furnish two relations each between the four sets of unknowns, and by imposing these conditions on the solutions,

Eqs. (3.31) through (3.36), we obtain all the necessary relations.

For $u_1 = u_2$ at $y = y_1$, we have

$$\sum_{n=1}^{\infty} \sin k_n x \Big\{ C_{1n}[-2k_n y_1 e^{k_n y_1} - 2 \sinh k_n y_1]$$

$$+ D_{1n}[2 \sinh k_n y_1 + 2k_n y_1 \cosh k_n y_1]$$

$$+ C_{2n} e^{k_n h}[2 \sinh k_n(h+y_1) + 2k_n(h+y_1) e^{k_n(h+y_1)}]$$

$$- D_{2n} e^{k_n h}[2k_n y_1 \cosh k_n(h+y_1) + 2 \sinh k_n(h+y_1)$$

$$+ 2k_n h(k_n h + k_n y + 1) e^{k_n(h+y_1)}]\Big\} = 0 \qquad (3.39)$$

For $v_1 = v_2$ at $y = y_1$, we have

$$\sum_{n=1}^{\infty} \cos k_n x \Big\{ C_{1n}[2k_n y_1 e^{k_n y_1} - 2 \sinh k_n y_1] - D_{1n} 2k_n y_1 \sinh k_n y_1$$

$$- C_{2n} e^{k_n h}\Big[2k_n(h+y_1) e^{k_n(h+y_1)} - 2 \sinh k_n(h+y_1)\Big]$$

$$+ D_{2n} e^{k_n h}\Big[2k_n^2 h(h+y_1) e^{k_n(y+y_1)} + 2k_n y_1 \sinh k_n(h+y_1)\Big]\Big\} = 0$$

$$(3.40)$$

The application of the boundary condition expressed by Eq. (3.38) yields two more relations:

$$\frac{4\eta_1}{a}\sum_{n=1}^{\infty} \sin k_n x \left\{ C_{1n} - 2k_n \cosh k_n y_1 - 2k_n^2 y_1 \, e^{k_n y} \right]$$

$$+ \; D_{1n}\left[2k_n^2 y_1 \sinh k_n y_1 + 2k_n \cosh k_n y_1\right]\Big\}$$

$$+ \; \frac{4\eta_2}{a}\sum_{n=1}^{\infty} \sin k_n x \left\{ C_{2n} e^{k_n h}\left[2k_n \cosh k_n (h+y_1)\right.\right.$$

$$+ \; \left. 2k_n^2 (h+y_1) e^{k_n (h+y_1)}\right] - D_{2n} e^{k_n h}\left[2k_n \cosh k_n (h+y_1)\right.$$

$$+ \; \left.\left. 2k_n^2 y_1 \sinh k_n (h+y_1) + 2k_n^2 h\left(k_n (h+y_1)+1\right) e^{k_n (h+y_1)}\right]\right\}$$

$$= \; \frac{4\eta_2}{a}\sum_{n=1}^{\infty} \sin 2\beta \cos k_n x \left\{ C_{2n} e^{k_n h} \; 2k_n e^{k_n (h+y_1)}\right.$$

$$\left. - \; D_{2n} e^{k_n h}\left[2k_n \sinh k_n (h+y_1) + 2k_n^2 h \; e^{k_n (h+y_1)}\right]\right\}$$

$$- \; \frac{4\eta_1}{a}\sum_{n=1}^{\infty} \sin 2\beta \cos k_n x \left\{ C_{1n} 2k_n e^{k_n y_1} - D_{1n} 2k_n \sinh k_n y_1 \right\}$$

$$+ \; (\rho_1 - \rho_2)\, g\, (h_1 + y_1) \sin 2\beta \qquad (3.41)$$

and

$$\frac{4\eta_2}{a}\sum_{n=1}^{\infty}\cos k_n x\left\{C_{2n}e^{k_n h}\left[2k_n\left(k_n(h+y_1)+1\right)e^{k_n(h+y_1)}\right.\right.$$

$$-\ 2k_n\cosh k_n(h+y_1)\Big] - D_{2n}e^{k_n h}\Big[2k^2h\left(k_n(h+y_1)+1\right)e^{k_n(h+y_1)}$$

$$\left.\left.+\ 2k_n^2y_1\cosh k_n(h+y_1)+2k_n\sinh k_n(h+y_1)\right]\right\}$$

$$-\ \frac{4\eta_1}{a}\sum_{n=1}^{\infty}\cos k_n x\left\{C_{1n}\left[2k_n(k_ny_1+1)e^{k_ny_1}-2k_n\cosh k_ny_1\right]\right.$$

$$\left.-\ D_{1n}\left[2k_n^2y_1\cosh k_ny_1+2k_n\sinh k_ny\right]\right\}$$

$$=\ \frac{4\eta_2}{a}\sum_{n=1}^{\infty}\cos 2\beta\cos k_n x\left\{C_{2n}e^{k_nh}\ 2k_ne^{k_n(h+y_1)}\right.$$

$$\left.-\ D_{2n}e^{k_nh}\left[2k_n\sinh k_n(h+y_1)+2k^2h\ e^{k_n(h+y_1)}\right]\right\}$$

$$-\ \frac{4\eta_1}{a}\sum_{n=1}^{\infty}\cos 2\beta\cos k_n x\left\{C_{1n}\ 2k_ne^{k_ny_1}-D_{1n}\ 2k_n\sinh k_ny\right\}$$

$$+\ (\rho_1-\rho_2)\,g\,(h_1+y_1)\cos 2\beta \tag{3.42}$$

4. NUMERICAL SOLUTION

Equations (3.39) through (3.42) provide four relations in four sets of unknowns in terms of infinite sums. If we were by some scheme able to solve for these constants, i.e., C_{1n}, C_{2n}, D_{1n}, and D_{2n}, $n = 1,2,3,\ldots\infty$, then we immediately could determine all the velocities and hence the motion of the interface. The process of finding these unknowns is not simple, except in the trivial case for which $y_1 = h_1$,

then all the constants are zero, and there is no motion.

The fact that we have four infinite sets of unknowns brings to mind the idea of completeness, as in the case of determining the unknown constants in the Fourier series expansion of functions; this method will not be adequate, because some of the integrals generated will be quite unmanageable, especially when the initial perturbation is sinusoidal. To illustrate, suppose

$$y_1 = y_o \sin \frac{\pi x}{a} ,$$

then a typical integral would be

$$\sum_{n=1}^{\infty} C_{1n} \int_0^a \cos k_n x \cosh \left[k_n \left(h + y_o \sin \frac{\pi x}{a} \right) \right] \cos k_n x \, dx .$$

It is unlikely that a closed-form answer for this integral could be found, though an answer in terms of Bessel functions cannot be ruled out. A disadvantage of this method is that it could not be applied more than once, as it would not give the analytical expression for the new interface to allow continuation of the process.

The other method for solving these unknowns is the generation of as many equations as there are unknowns. However, an infinite number of equations has to be ruled out. Hence, the following approximation procedure is used. Since, as was shown above, a knowledge of the constants of integration is sufficient for the determination of the velocity field, the following numerical procedure is proposed, by which these constants may be evaluated:

1) Since a perturbation at the interface is necessary to initiate the instability, we assume at time $t = t_o$ an initial perturbation of the form $y = -h_1 - b \cos \pi x/a$.

2) The infinite sums appearing in Eqs. (3.39) through (3.42) are truncated to N terms. This will introduce an error in the boundary conditions at the interface, but not in the solutions of the differential equations. All of the errors introduced are of the form

$$Q_1(x) = Q_2(x) + \epsilon(x) \tag{4.1}$$

where Q represents either velocities or stresses, and ϵ is the error. This error can be made as small as desired by increasing N.

3) The truncation of the infinite sums to N terms reduces the number of unknowns to 4N. We could choose N points along the interface, then the truncated forms of Eqs. (3.39) through (3.42) would generate 4N equations which would satisfy the boundary conditions at the N points. Subsequently these equations could be solved for the 4N unknowns. This method was tried, and it yielded excellent results at the selected points of the interface, i.e., it preserved the continuity of velocities and stresses as required by the boundary conditions. However, when velocities were calculated at random points along the interface, unacceptable results were obtained. The reason for this is that the truncated equations had been forced to be satisfied at N points along the interface, but no control whatever had been exercised

over the functions in the intervals between the N points.

In order to both satisfy the boundary conditions at the N points and to control the behavior of the truncated functions in-between points, we use the following procedure: The homogeneous equations (3.39) and (3.40) are fitted at N points and thereby generate 2N equations in 4N unknowns. Thus a matrix relation between the constants is established. This matrix relation is then used in the truncated form of Eqs. (3.41) and (3.42) to reduce the number of unknowns to 2N. Next, M points (M > 2N) along the interface are used to fit the resulting equations, in the least-square sense, in order to determine the 2N unknowns. The mathematical details of this procedure are given in Appendix B.

4) Once the unknown constants are determined, the velocity fields are known (including velocities at the interface), and points on the interface may be advanced according to the explicit relation,

$$\begin{aligned} x_{n+1} &= x_n + u_n \Delta t \\ y_{n+1} &= y_n + v_n \Delta t \end{aligned} \tag{4.2}$$

where Δt is a time increment, or by the implicit relation that accounts for changes in velocity,

$$\begin{aligned} x_{n+1} &= x_n + \tfrac{1}{2}(u_{n+1} + u_n)\Delta t \\ y_{n+1} &= y_n + \tfrac{1}{2}(u_{n+1} + u_n)\Delta t \end{aligned} \tag{4.3}$$

Hence a new interface is established, and we will be at Step 1). The whole process may be repeated until we have advanced the interface the total time desired. In the present investigation a Fourier fit to the discrete points along the interface was carried out to approximate a new functional relation for the interface.

The above method is referred to as a boundary method in the literature. A boundary method refers to the numerical procedures whereby the differential equations are satisfied but not the boundary condition, or vice versa.

5. NUMERICAL RESULTS FOR SMALL PERTURBATIONS

In the present investigation, the solution to the linear problem of small perturbation was used to test the validity of the method. The linear theory predicts that an infinitesimal sinusoidal displacement, $y = y_o \cos x$, with an initial amplitude y_o, grows as

$$y_o = A\, e^{pt} \tag{5.1}$$

To test that this method does indeed yield comparable results for a small perturbation, a case where the amplitude of the initial disturbance was $0.01\ h_1$ was simulated, and the growth of the amplitude was calculated. Table I shows that y_o does indeed grow exponentially at both trough and crest, in perfect agreement with the linear theory. The small differences between the p's for trough and crest are a measure of the deviation of the result from the linear theory. When the viscosity ratio was much larger than the ratio used in preparing Table I, the agreement was almost

exact. The graph in Fig. 3 depicts the linear case for a viscosity ratio $\eta_1/\eta_2 = 100$; it clearly shows the identical growth of the amplitude on both sides of the stagnation point.

A further check on the method is as follows: It is obvious that for small perturbation the interface will deviate little from the initially assumed sinusoidal shape; hence, the Fourier coefficients of the higher frequencies in the interface must be small with respect to the first coefficient. This indeed was verified numerically.

6. NUMERICAL RESULTS FOR LARGE PERTURBATIONS

For large perturbations there are no known solutions with which to compare. Therefore we can only demonstrate the physical consistency of the solutions.

The graphs in Figs. 4 and 5 depict the development of an initial large perturbation of the form

$$y = -h_1 - b \cos \frac{\pi x}{a}$$

The system has the following physical properties:

$a = 2.0 \times 10^5$ cm, the length of the model

$h_1 = 1.0 \times 10^5$ cm, the thickness of the model

$h = 2.0 \times 10^5$ cm, the total thickness of the model

$\eta_1 = 10^{19}$ poise, the viscosity of the top layer

$\eta_2 = 10^{17}$ poise, the viscosity of the bottom layer

$\rho_1 = 2.2$ gm/cm^3, the density of the top layer

$\rho_2 = 2.0$ gm/cm^3, the density of the bottom layer

$b = 1.0 \times 10^4$ cm, the amplitude of the initial perturbation .

Since the material was incompressible, conservation of volume was expected for the results to be acceptable. A comparison was made of the volume of the crest with the volume of the trough. The error in the volume balance was always less than 1.0%.

The graphs in Fig. 4 show the stages of development of the interface. Each curve is obtained after advancing the interface five time-steps. The velocity field is that of the system after the first five time-steps. The velocity in the x direction along the interface was always negative, but the velocity field was indeed that which was expected of an incompressible fluid.

Figure 5 shows the initial interface, the new interface, and the velocity field after twenty time-steps. The graphs clearly show the conservation of volume, and that as the perturbation grows the velocities get larger; this, of course, is in agreement with the physical situation. Large perturbation imply large forces, which imply large acceleration, which imply large velocities. If the velocity field graphs of Figs. 4 and 5 were superimposed on each other, then the instantaneous stagnation point would be observed to move to the left.

To further make the results of the method plausible, a case where $\rho_1 < \rho_2$ was tried. The results are shown in Fig. 6. It clearly shows that the perturbation dies out.

The calculated velocities of the system were of the order of one centimeter/year. Hence, we may establish a posteriori argument for neglecting forces arising from quadratic terms in velocities compared to viscous forces.

$$\frac{F_v}{F_\eta} = \frac{\rho\left(\frac{\partial v}{\partial t} + v \cdot \nabla v\right)}{\eta \nabla^2 v}$$

$$\frac{F_v}{F_\eta} = \frac{\rho\left(\frac{\partial v}{\partial t} + v^2\right)}{\eta \nabla^2 v} \approx 10^{-9}$$

where F_v and F_η are forces arising from velocities and viscosities, respectively. The ratios in the last equation are indeed small, and the neglect of the total derivatives of velocities in the Navier-Stokes equation is justified.

7. CONCLUSIONS

In this paper we used finite sine and cosine transforms to obtain a solution for the Navier-Stokes equation for the case of a Taylor instability in two viscous incompressible fluids horizontally stratified. Nonlinear terms that appear in the boundary conditions were retained. The inclusion of these nonlinear terms allows the application of large perturbation and becomes more important as the perturbation grows and develops steeper flanks (Daneš, 1964).

We apply this method for the evolution of salt-domes by considering two strata of finite thickness, rigid base, and upper surface of overburden with no slip at the interface. We believe such conditions are most amenable to laboratory examination (Ramberg, 1968a). We find that our results are physically consistent. We also find that the initial rise of the salt-dome is fast, in agreement with results obtained by Berner et al, 1972. The velocity field at different times are calculated. Using

these velocity fields, particle paths may be calculated, and hence shear stresses may be found (Ramberg, 1975; Dixon, 1975). Other geological and geophysical phenomena, such as the evolution of granitic and gneissic domes, anticline cases, and magma intrusions (Gibb, 1976) are amenable to solution using the method reported here.

0 0 0 0 4 9 0 2 4 4 5

ACKNOWLEDGMENTS

One of us (O.B.D.) is grateful to Professors D. A. Shirley and H. A. Shugart of the Materials and Molecular Research Division of Lawrence Berkeley Laboratory, and Professors Abdus Salam and P. Budini of the International Centre for Theoretical Physics, for their kind hospitality during the time when parts of this work was done.

Work was supported by the U. S. Energy Research and Development Administration.

APPENDIX A
CONTINUITY CONDITIONS AT THE INTERFACE

The condition of no slip implies that there can be no relative velocity between two different particles at the same point of the interface; this condition may be expressed as

$$u_1 = u_2 \quad , \qquad v_1 = v_2 \quad . \tag{A.1}$$

The continuity of stresses follows from the fundamental definition of action-reaction. If we assume a thin element of matter containing the interface, and attach a coordinate system ξ,η to the interface, then the continuity of stresses may be expressed as

$$\sigma_\eta^{(1)} = \sigma_\eta^{(2)} \quad , \qquad \sigma_{\eta\xi}^{(1)} = \sigma_{\eta\xi}^{(2)} \quad . \tag{A.2}$$

Equation (A.2) may be transformed to an x,y coordinate by using equilibrium conditions on a free-body diagram, as seen in Fig. 8. From the law of equilibrium, i.e., $\Sigma F = 0$, we have on an element of area ds

$$\sigma_\eta ds = \sigma_y \cos^2 \beta ds + \sigma_x \sin^2 \beta ds - \sigma_{xy} \sin \beta \cos \beta ds - \sigma_{yx} \sin \beta \cos \beta ds \tag{A.3}$$

and

$$\sigma_{\eta\xi} ds = \sigma_y \cos \beta \sin \beta ds - \sigma_x \sin \beta \cos \beta ds + \sigma_{xy} \cos^2 \beta ds - \sigma_{xy} \sin^2 \beta ds \tag{A.4}$$

Equations (A.3) and (A.4) hold for either medium, hence, by using Eqs. (A.2) and the fact that $\sigma_{xy} = \sigma_{yx}$, we have

$$\sigma_x^{(1)} + \sigma_y^{(1)} - \left(\sigma_x^{(1)} - \sigma_y^{(1)}\right) \cos 2\beta - 2\sigma_{xy}^{(1)} \sin 2\beta$$

$$= \sigma_x^{(2)} + \sigma_y^{(2)} - \left(\sigma_x^{(2)} - \sigma_y^{(2)}\right) \cos 2\beta - 2\sigma_{xy}^{(2)} \sin 2\beta \tag{A.5}$$

and

$$\left(\sigma_y^{(1)} - \sigma_x^{(1)}\right) \sin 2\beta + 2\sigma_{xy}^{(1)} \cos 2\beta = \left(\sigma_y^{(2)} - \sigma_x^{(2)}\right) \sin 2\beta + 2\sigma_{xy}^{(2)} \cos 2\beta \tag{A.6}$$

By means of relations between stresses, pressure, and angular deformation, we have for an incompressible material,

$$(P_2 - P_1) \sin 2\beta = \eta_1 \left(\frac{\partial u_1}{\partial y} + \frac{\partial v_1}{\partial x}\right) - \eta_2 \left(\frac{\partial u_2}{\partial y} + \frac{\partial v_2}{\partial x}\right) \tag{A.7}$$

and

$$(P_2 - P_1) \cos 2\beta = 2\eta_2 \frac{\partial v_2}{\partial x} - \eta_1 \frac{\partial u_1}{\partial y} \tag{A.8}$$

These are the boundary conditions used in Section 3 equations (3.38).

APPENDIX B

DETERMINATION OF THE CONSTANTS OF INTEGRATION BY THE LEAST SQUARE METHOD

Equations (3.39) through (3.42) are all of the same form and may be written as follows:

$$\sum_{n=1}^{2N} A_n f_{1,n} = \sum_{n=1}^{2N} B_n g_{2,n} \tag{B.1}$$

$$\sum_{n=1}^{2N} A_n g_{1,n} = \sum_{n=1}^{2N} B_n g_{2,n} \tag{B.2}$$

$$\sum_{n=1}^{2N} A_n h_{1,n} + \sum_{n=1}^{2N} B_n h_{2,n} = F_1 \tag{B.3}$$

$$\sum_{n=1}^{2N} A_n P_{1,n} + \sum_{n=1}^{2N} B_n P_{2,n} = F_2 \tag{B.4}$$

Equations (B.1) and (B.2) were fitted at N number of x's, and a matrix relation between the A's and the B's was established, i.e.,

$$A_k = \sum_{n=1}^{2N} \alpha_{kn} B_n \quad . \tag{B.5}$$

Equation (B.5) was then substituted in Eqs. (B.3) and (B.4) to obtain

$$\sum_{k=1}^{2N} \sum_{n=1}^{2N} \alpha_{kn} B_n h_{1,k} + \sum_{n=1}^{2N} B_n h_{2,n} = F_1$$

or

$$\sum_{n=1}^{2N} B_n \sum_{k=1}^{2N} \alpha_{kn} h_{1,k} + h_{2,n} = F_1 \quad ,$$

and

$$\sum_{n=1}^{2N} B_n \sum_{k=1}^{2N} \alpha_{kn} P_{1,k} + P_{2,n} = F_2 \quad .$$

Let

$$h_{3,n} = \sum_{k=1}^{2N} \alpha_{kn} h_{1,k} + h_{2,n} \quad ,$$

and

$$P_{3,n} = \sum_{k=1}^{2N} \alpha_{kn} P_{1,k} + P_{2,n} \quad ;$$

then

$$\sum_{n=1}^{2N} B_n h_{3,n} = F_1 \quad , \tag{B.6}$$

$$\sum_{n=1}^{2N} B_n P_{3,n} = F_2 \quad . \tag{B.7}$$

The least square method was used on Eqs. (B.6) and (B.7) in the following way:

We let

$$\sum_{n=1}^{2N} B_n h_{3,n}(x) - F_1(x) = \epsilon_1(x) \quad , \tag{B.8}$$

$$\sum_{n=1}^{2N} B_n P_{3,n}(x) - F_2(x) = \epsilon_2(x) \quad . \tag{B.9}$$

where ϵ_1 and ϵ_2 are the errors at each of M points along the interface. The sum of the squares of the errors were minimized with respect to the

B's to obtain

$$\sum_{n=1}^{2N} B_n \left(\sum_{\ell=1}^{M} h_{3,n}\, h_{3,\ell} + P_{3,n}\, P_{3,\ell} \right) = \sum_{\ell=1}^{M} \left(F_1\, h_{3,\ell} + F_2\, P_{3,\ell} \right) \quad . \tag{B.10}$$

REFERENCES

Allred, J.C. and Blount, G.H., 1954. Experimental studies of Taylor instability; Los Alamos Scientific Laboratory Report LA-1600, pp. 8-9.

Bellman, R., and Pennington, R.H., 1952. Effects of surface tension and viscosity on Taylor instability; Princeton University Report, Project Matterhorn.

Berker, R., 1963. Integration des equations du mouvement d'un fluide visqueux incompressible; Handbuch der Physik, Ed. S. Flügge (Springer, Berlin, vol. 8).p

Berner, H., Ramberg, H. and Stephansson, O., 1972. Diapirism in theory and experiment; Tectonophysics 15: 197-218.

Biot, M.A., 1959. The influence of gravity on the folding of a layered viscoelastic medium under compression; J. Franklin Inst. 267: 211-228.

Biot, M.A., 1966. Theory of folding of stratified viscoelastic media and its implication in tectonics orogenesis; Bull. Geol. Soc. Am. 72: 1595-1960.

Biot, M.A. and Odé, H., 1965. Theory of gravity instability with variable overburden and composition. Geophysics 30: 213-227.

Birkhoff, G.D., and Ingraham, R., 1952. Harvard University Report.

Chandrasekhar, S., 1955. The character of the equilibrium of an incompressible heavy viscous fluid of variable density; Proceedings Cambridge, Phil. Soc. 51: 162-178.

Daneš, Z.F., 1964. Mathematical formulation of salt-dome dynamics; Geophysics 29: 214-224.

Dixon, J.M., 1975. Finite strain and progressive deformation in models of diapiric structures; Tectonophysics 28: 189-124.

Erdelyi, A., ed. Bateman Manuscript Project, Table of Integral Transforms, Vol. 1 (McGraw-Hill, New York, 1954), Chapters I and II.

Gibb, F.G., 1976. Ultrabasic rocks of Rhum and Skye: the nature of parent magma; J. Geol. Soc. London 132: 209-222.

Harrison, W.J., 1908. The influence of viscosity on the oscillations of superposed fluids; Proceedings London Math. Soc. Ser. 3: 6, 396-405.

Lamb, H., 1945. Hydrodynamics (Dover, New York, 620 pp.)

Landau, L.D., and Lifshitz, E.M., 1959. Fluid Mechanics (Addison-Wesley, Reading, Massachusetts, pp. 47-53).

Odé, H., 1966. Gravitational instability of a multilayered system of high viscosity; Verh. K. Ned. Akad. Wet. Reeks 1, 24: 96.

Parker, T.J., and McDonell, A.M., 1955. Model studies of salt dome tectonics; Bull. Am. Assoc. Petr. Geol. 39: 2384-2471.

0 0 0 0 4 9 0 2 4 4 9

Ramberg, H., 1967. Gravity Deformation and the Earth's Crust as Studied by Centrifugal Models (Academic Press, London, 214 pp.).

Ramberg, H., 1968a. Fluid dynamics of layered systems in the field of gravity; a theoretical basis for certain global structures and isostatic adjustment; Phys. Earth Planet. Inter. 1: 63-87.

Ramberg, H., 1968b. Instability of layered systems in the field of gravity; Phys. Earth Planet. Inter. 1: 427-474.

Ramberg, H., 1972a. Experimental and theoretical study of salt-dome evolution; UNESCO, 1972, Geology of saline deposits. Proceedings Hanover Symposium, 1968 (Earth Sciences, 7).

Ramberg, H., 1972b. Theoretical models of density stratification and diapirism in the earth. J. Geophys. Research 77: 877-889.

Ramberg, H., 1975. Particle paths, displacement and progressive strain applicable to rocks. Tectonophysics 28: 1-37.

Rayleigh, Lord, 1883. Incompressible heavy fluid of variable density, Proceedings London Math. Soc. 17: 170-177.

Streeter, V.L., 1948. Fluid Dynamics (McGraw-Hill, New York, pp. 208-223).

Taylor, G., 1950. The instability of liquid surface when accelerated in a direction perpendicular to their planes; Part I, Proceedings Royal Soc. London, Series A: 201: 192-196.

TABLE I. Growth of trough and crest.

Trough				Crest			
t	$y_o(t)/A$	$pn\Delta t$	p	t	$y_o(t)/A$	$pn\Delta t$	p
Δt	1.3055	0.266	0.266	Δt	1.2992	0.262	0.262
$2\Delta t$	1.7093	0.536	0.268	$2\Delta t$	1.6899	0.524	0.262
$3\Delta t$	2.2440	0.808	0.269	$3\Delta t$	2.1990	0.788	0.263
$4\Delta t$	2.9532	1.082	0.271	$4\Delta t$	2.8604	1.051	0.263
$5\Delta t$	3.8966	1.360	0.272	$5\Delta t$	3.7168	1.312	0.262
$6\Delta t$	5.1560	1.640	0.273	$6\Delta t$	4.8205	1.569	0.261

0 0 0 0 4 9 0 2 4 5 0

FIGURE CAPTIONS

Fig. 1. Geometry of two viscous layers on a rigid base.

Fig. 2. Initial perturbation and boundary conditions.

Fig. 3. The development of the interface for an initial small perturbation. Curve (1) represents the initial interface; curves (2), (3), and (4) represent the shapes of the interfaces at 30,000, 120,000 and 180,000 years respectively.

Fig. 4. The development of the interface for an initial larger perturbation. Curve (1) represents the initial interface; curves (2), (3), and (4) represent the shapes of the interface at 60,000, 120,000 and 168,000 years respectively. The vectors represent the velocity field at 30,000 years.

Fig. 5. The velocity and the interface for the initial perturbation of Fig. 4 after 120,000 years.

Fig. 6. Stable case where material of low density is on top of material of high density. Curve (1) represents the initial interface; curves (2) and (3) represent the interface at 60,000 and 120,000 years respectively.

Fig. 7. Geometry of interface for large perturbation.

Fig. 8. Free-body diagram of stress components.

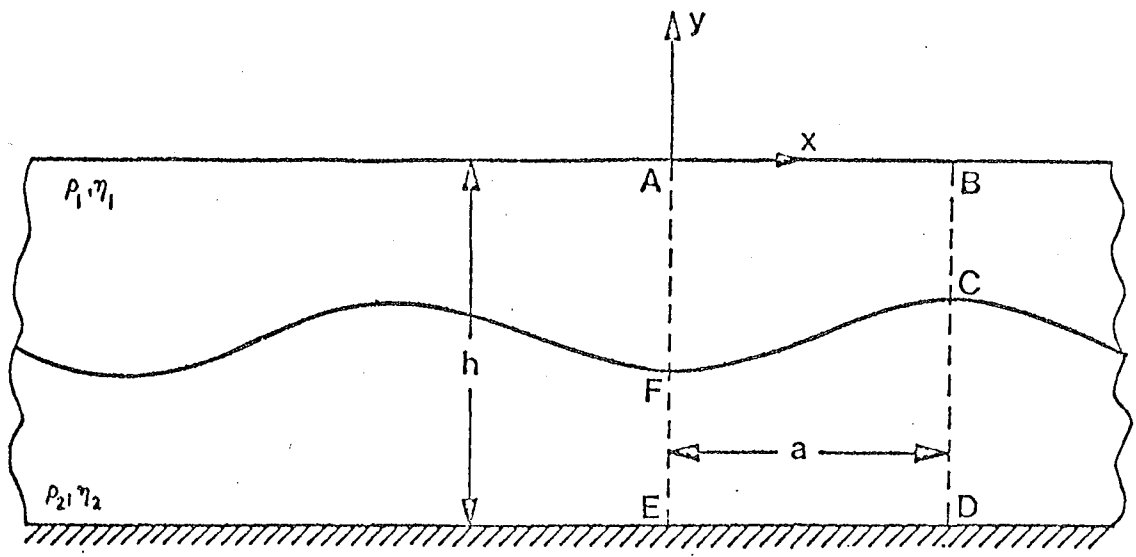
y
x
A
B
C
F
E
D
h
a
ρ_1, η_1
ρ_2, η_2

FIG. I

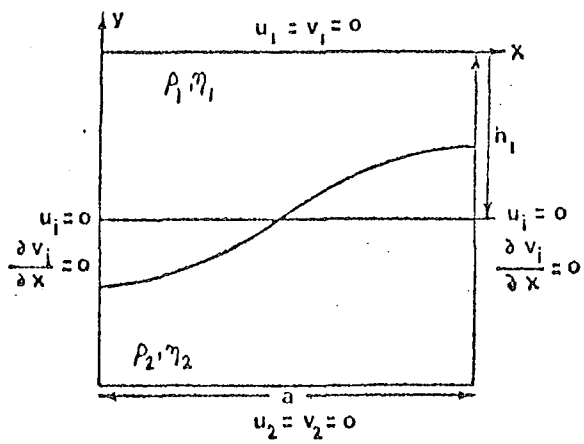
y
x
$u_1 = v_1 = 0$
ρ_1, η_1
h_1
$u_i = 0$
$\frac{\partial v_i}{\partial x} = 0$
$u_i = 0$
$\frac{\partial v_i}{\partial x} = 0$
ρ_2, η_2
a
$u_2 = v_2 = 0$

FIG. II

0 0 0 0 4 9 0 2 4 5 1

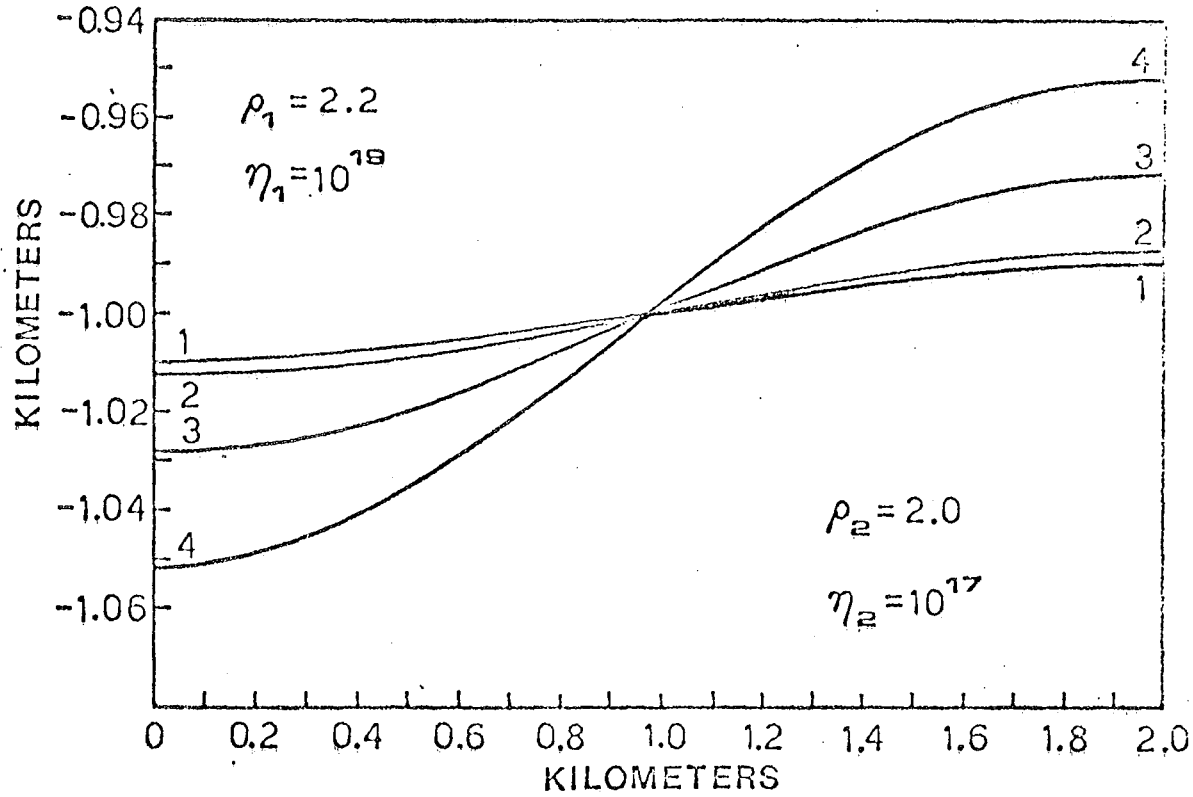

FIG. III

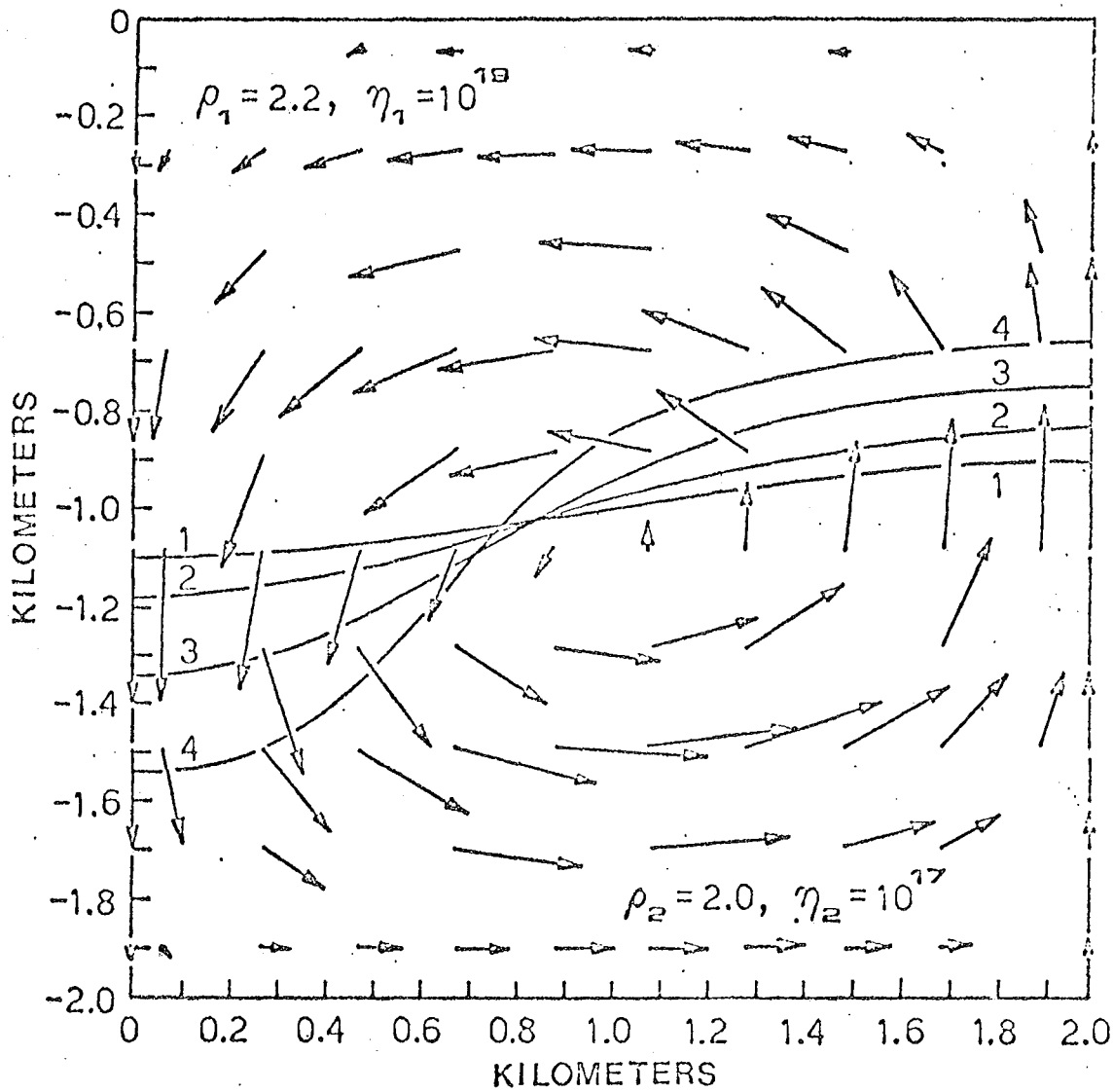
$\rho_1 = 2.2,\ \eta_1 = 10^{19}$
$\rho_2 = 2.0,\ \eta_2 = 10^{17}$
KILOMETERS
KILOMETERS
0
-0.2
-0.4
-0.6
-0.8
-1.0
-1.2
-1.4
-1.6
-1.8
-2.0
0
0.2
0.4
0.6
0.8
1.0
1.2
1.4
1.6
1.8
2.0
1
2
3
4

FIG. IV

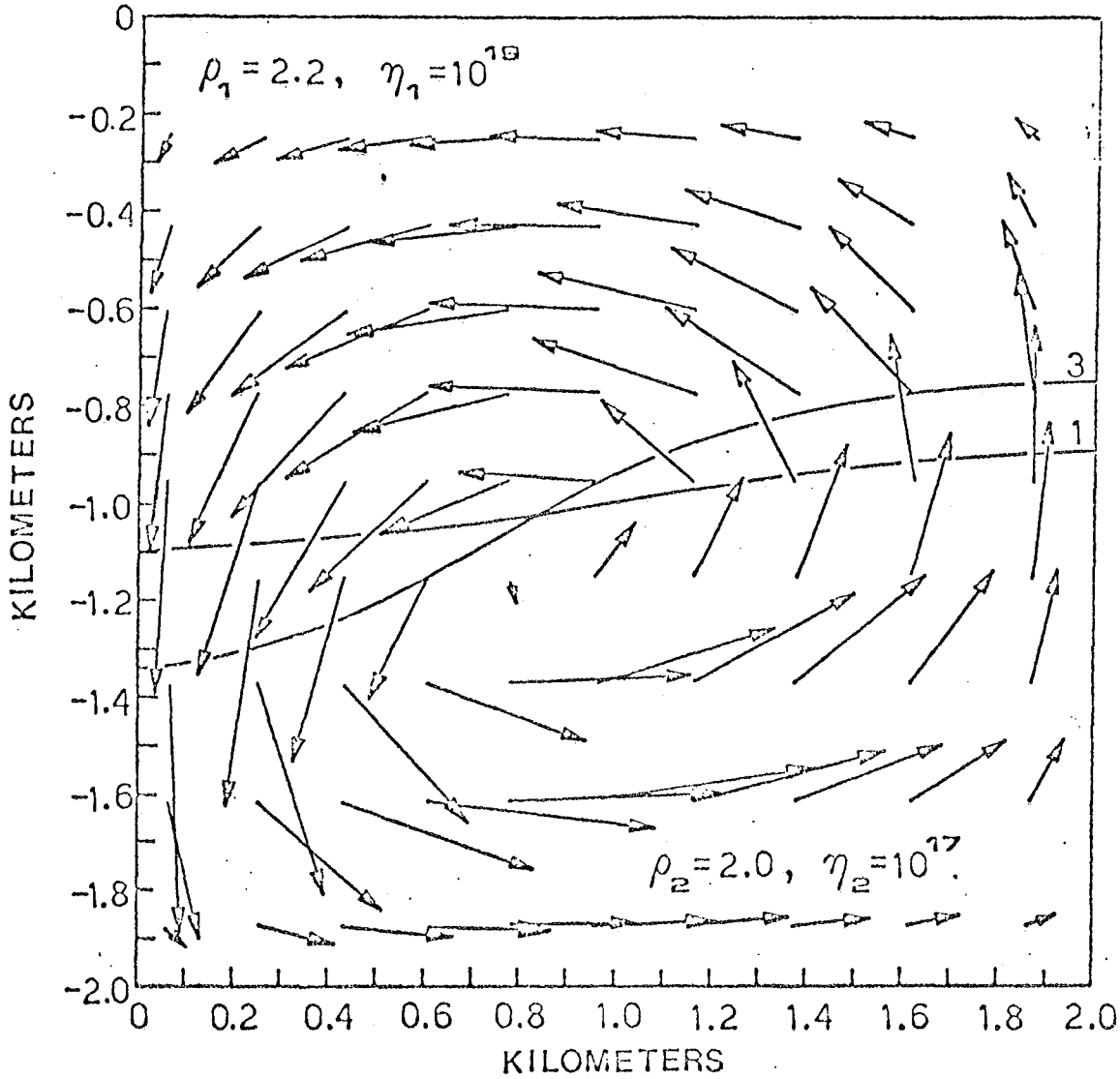
$\rho_1 = 2.2$, $\eta_1 = 10^{18}$
$\rho_2 = 2.0$, $\eta_2 = 10^{17}$
3
1
KILOMETERS
KILOMETERS
0
-0.2
-0.4
-0.6
-0.8
-1.0
-1.2
-1.4
-1.6
-1.8
-2.0
0
0.2
0.4
0.6
0.8
1.0
1.2
1.4
1.6
1.8
2.0

FIG. V

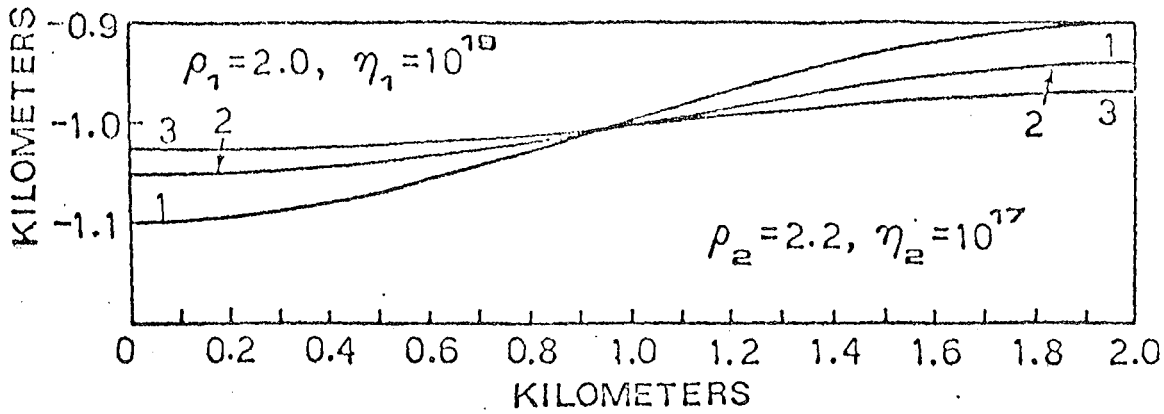

FIG. VI

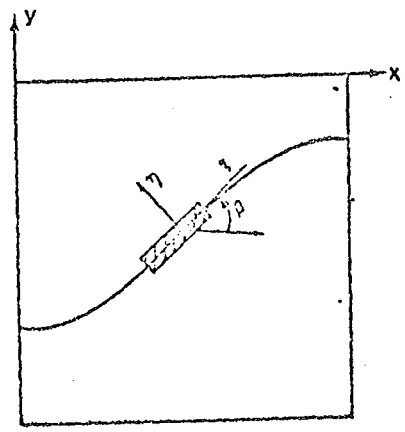

FIG. VII

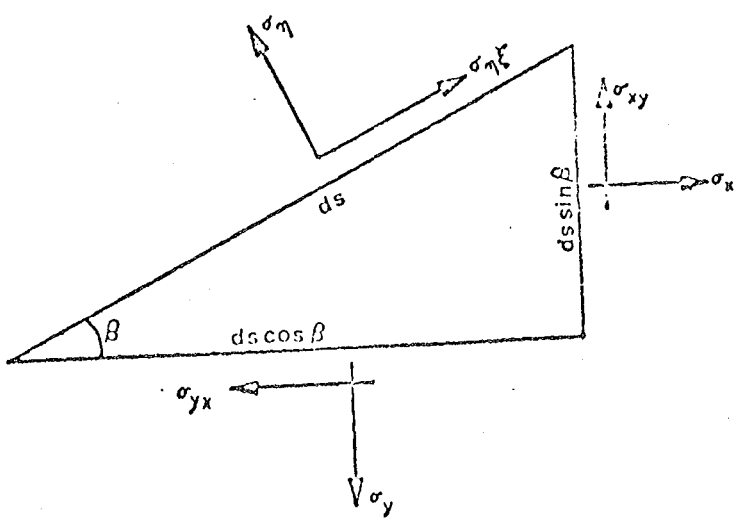

FIG. VIII

This report was done with support from the United States Energy Research and Development Administration. Any conclusions or opinions expressed in this report represent solely those of the author(s) and not necessarily those of The Regents of the University of California, the Lawrence Berkeley Laboratory or the United States Energy Research and Development Administration.

0 0 0 0 4 5 0 2 2 9 4